Azimuthal asymmetry of black particles in high-energy interactions—evaporation model revisited

Dipak Ghosh, Sharmila Sarkar, Krishnadas Purkait
and Asok Kumar Mallick

High Energy Physics Division, Department of Physics, Jadavpur University,
Calcutta-700 032, India

Abstract : Azimuthal anisotropy of target fragments in C^{12}–Em interactions at 4.5 GeV/c/n and O^{16}–Em interactions at 60 GeV/c/n is investigated here. The evaporation model fails to explain the experimental data. The model of local heating is found to describe the data satisfactorily.

Keywords : Azimuthal anisotropy, target fragments, local heating model

PACS No. : 25.75.–q

1. Introduction

In the cases of relativistic nucleus-nucleus inelastic interactions at high energies a large part of the total cross section is due to multiparticle production. It is also found that the characteristics of disintegration are functions of number of interacting nucleous of the projectile and the target nuclei and therefore, also functions of the mass of the colliding nuclei. After interaction, a spectator piece of the target is formed and if the impact parameter is sufficiently large, a spectator piece of the projectile is also formed [1–4].

According to Additive Quark model, two incoherent 'wounded' quarks are responsible for particle production phenomena in nucleus-nucleus inelastic interactions at high energies [5]. In the Dual-Parton model, exchange of colours is the first step in inelastic hadronic collisions at high energies. In the intermediate state, two chains are formed for every exchange of colours. These chains which fragment into hadrons

are attached to different objects in the projectile and the target nuclei [5]. According to evaporation model, black particles are emitted from a system in statistical equilibrium and the distribution of those particles are expected to be isotropic in the angular range [6].

Here, we mention a few defficiencies of evaporation model. Sullivan *et al* [7], in their plastic detector experiment Kullberg and Otterlund [8], in their cosmic ray experiment showed deviations from evaporation model. Warwick *et al*-[9] and Gosset *et al* [10] also observed deviations from conventional evaporation scenario.

It is also found from the study of the energy spectrum of slow particles that the existence of inequilibrium states exist in the system of nucleons inside an excited nucleus [6–11].

Powell *et al* [12] supposed local heating of the target nucleus. During collisions, some part or the whole of the target nucleus is affected. This affected part of the residual target nucleus is heated due to absorption of a part of the energy of the projectile. This is known as local heating model (LHM). In the cases of noncentral collisions, the residual target nucleus is an assembly of inhomogeneously heated nucleons which are in statistical equilibrium. In the cases of central collisions, the degree of homogeneity in heating of the nucleons of the residual target is significant and hence the statistical equilibrium in the excited residue is also significant. According to LHM, in the cases of noncentral collisions, those black particles which are near the surface of locally heated region and moving towards the surface of that region may escape residual target easily, whereas those black particles which are interior to the residual target after encountering a number of collisions, either can escape residual target or cannot escape residue due to lack of energy. In the cases of central collisions, as the affected region of the target nucleus is increased, the number of black tracks is also increased [12].

The recent revival of interest in studying azimuthal asymmetry in detail is connected with the observation of an intermittency effect in nucleus-nucleus inelastic interactions at high energies [13].

This paper reports an extensive study of the azimuthal asymmetry of black particles in C^{12}-Em and O^{16}-Em interactions at incident beam-momenta 4.5 GeV/c/n and 60 GeV/c/n respectively, in the light of LHM (local heating model).

2. Experimental data

The required data is obtained from NIKFIBR2 nuclear research emulsion plates (25 cm × 10 cm × 600 µm) irradiated horizontally with C^{12} or O^{16} beam from JINR synchrophasotron. Primary inelastic events of C^{12}-Em interactions and primary inelastic events of O^{16}-Em interactions are investigated here. We have classified the secondary particles in *b, g, s,* particles following the usual nuclear emulsion methodology.

(i) The emission tracks having a range < 3 mm and ionisation $I > 6I_0$ where I_0 is the plateau of ionisation value of the singly charged particles in the emulsion pellicle, are known as black (b) tracks.

(ii) The emission tracks having a range > 3 mm and ionisation $1.4I_0 < I < 6I_0$ are known as grey (g) tracks.

(iii) The tracks having ionisation $I < 1.4I_0$ and very long ranges are known as shower (s) tracks. The tracks with emission angle greater than 3° are considered here to exclude the contamination of projectile associated fast fragments.

Absemetova *et al* [14] showed from the data of the energy of the evaporated slow particles and the degree of excitation of the residual target nucleus that the maximum of the energy of the slow particles in the energy spectrum shifts towards the lower energies with the increase of the number of black-grey tracks. This phenomenon cannot be explained by cascade evaporative model (CEM).

3. Method of analysis

We have studied here the azimuthal asymmetry of black particles in non-overlapping equal width cos θ bins and in the entire cos θ range.

If the number of black tracks and grey tracks in an event be n_b and n_g respectively, then

$$N_h = n_b + n_g.$$

where N_h is the number of heavy ion tracks in the event. The events are divided into a few N_h intervals which are $(1 \leq N_h \leq 5)$, $(6 \leq N_h \leq 10)$, $(11 \leq N_h \leq 15)$, $(16 \leq N_h \leq 20)$. The non-overlapping cos θ bins are $(-1.0$ to $-0.6)$, $(-0.6$ to $-0.2)$, $(-0.2$ to $0.2)$, $(0.2$ to $0.6)$, $(0.6$ to $1.0)$.

For the events in a N_h interval, azimuthal asymmetry of black particles of the i-th event in the j-th cos θ bin is defined as,

$$W_{ij} = \frac{x_{ij} - y_{ij}}{x_{ij} + y_{ij}}.$$

where x_{ij} = number of black particles of the i-th event in the j-th cos θ bin whose azimuthal angles are less than 180°.

y_{ij} = number of black particles of the i-th event in the j-th cos θ bin whose azimuthal angles are greater than 180°. For the events of a given N_h interval average azimuthal asymmetry in the j-th cos θ interval is

$$\overline{W}_j = \frac{\sum_i W_{ij}}{N^*} \qquad i = 1 \text{ to } N^*.$$

where N^* is the total number of events in the j-th cos θ bin for a given N_h interval. As the degree of excitation of the target nucleus depends on N_h, we have taken N_h as a parameter of the event [14].

The above formulae are applied for calculating average azimuthal asymmetry for the events of each N_h interval in the entire $\cos\theta$ range.

4. Results and discussions

Figures 1(a) to 1(d) are asymmetry $(\overline{W})$ *vs* $\cos\theta$ graphs of ^{12}C-Em interactions at 4.5 GeV/n/c for different N_h intervals. Figures 1(e) to 1(g) are asymmetry $(\overline{W})$ *vs* $\cos\theta$
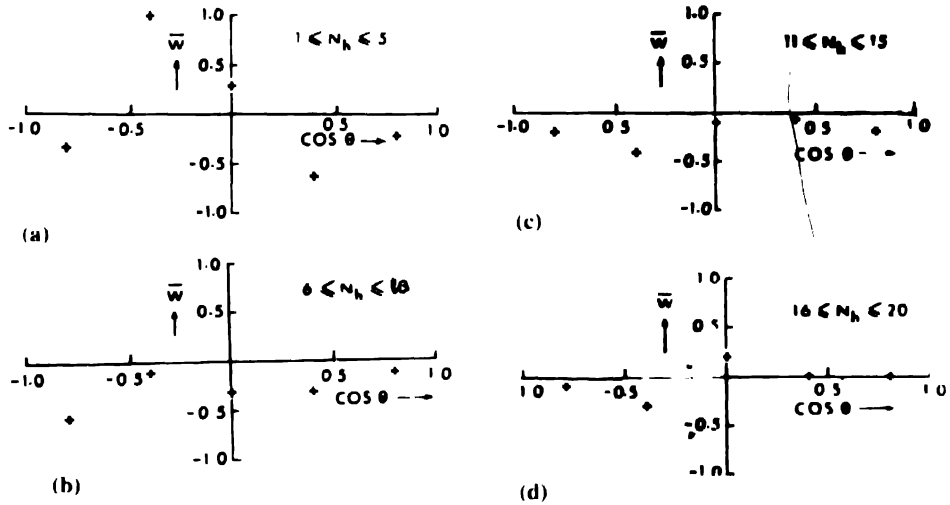

Figure 1. (a) to (d) are plots of $\overline{W}$ *vs* $\cos\theta$ graphs for ^{12}C-Em interactions at 4.5 GeV/c/n
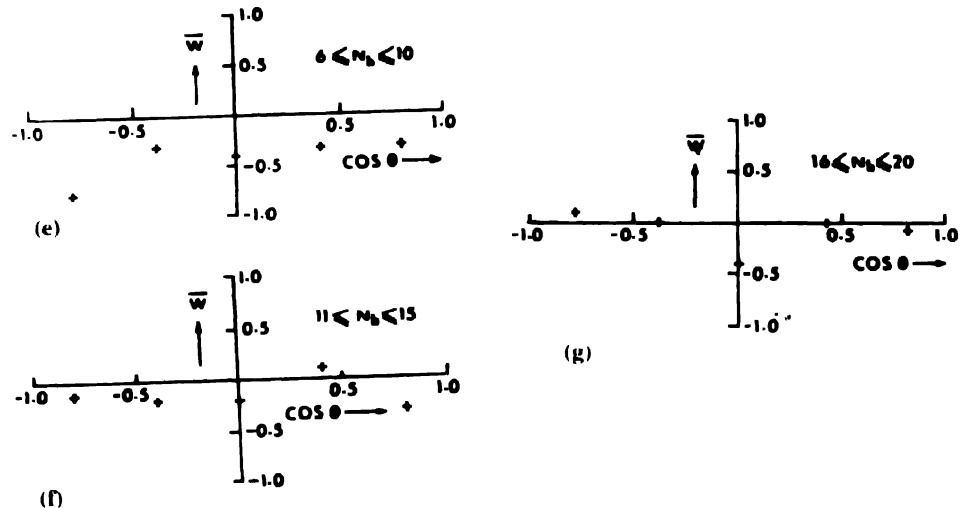
Figure 1. (e) to (g) are plots of $\overline{W}$ *vs* $\cos\theta$ graphs for ^{16}O-Em interactions at 60 GeV/c/n

graphs of ^{16}O-Em interactions at 60 GeV/n/c for different N_h intervals. It is seen from the graphs that with the increase of N_h, average azimuthal asymmetry decreases for both ^{12}C-Em and ^{16}O-Em interactions. It is also seen from the graphs 1(a) to 1(d) that

average azimuthal asymmetry of black particles in the $\cos\theta$ bins of forward emission angles ($\theta < 90°$) are much lower than those of in the backward emission angles ($\theta > 90°$).
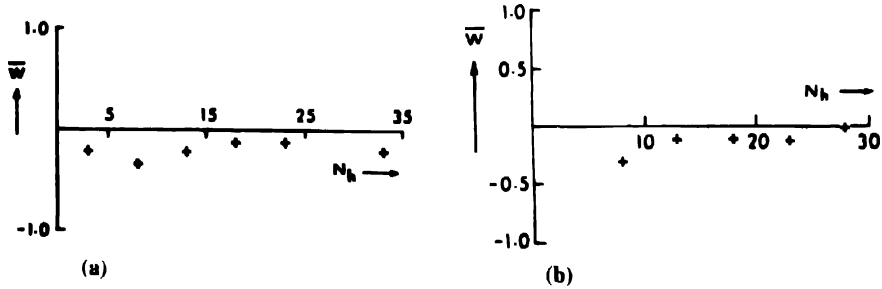
Figure 2. (a) and (b) are plots of $\overline{W}$ vs N_h graphs ^{12}C-Em interactions and ^{16}O-Em interactions at 4 5 GeV/c/n and 60 GeV/c/n respectively

Figures 2(a) and 2(b) are average azimuthal asymmetry vs N_h graphs for the entire $\cos\theta$ range for ^{12}C-Em interactions and ^{16}O-Em interactions at 4.5 GeV/c/n and 60 GeV/c/n respectively. Graphs 2(a) and 2(b) show that average azimuthal asymmetry of black particles decreases with the increase of N_h for both ^{12}C-Em and ^{16}O-Em interactions. Thus, this analysis shows that the average azimuthal asymmetry of black particles decreases with
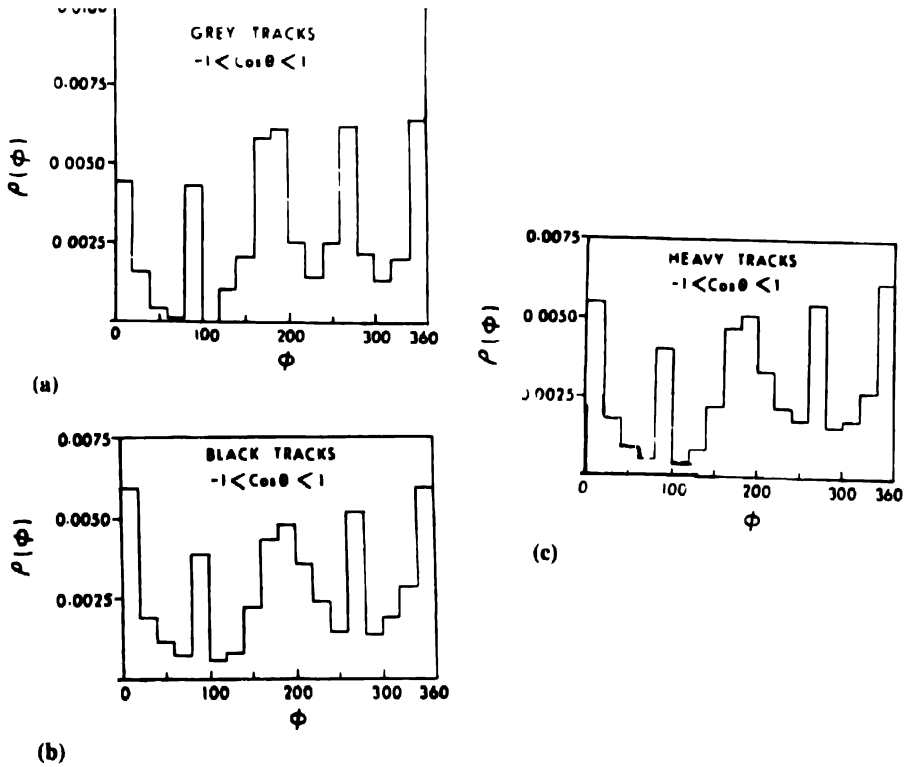
Figure 3. (a) to (c) are plots of $\rho(\phi)$ (for grey, black and heavy tracks respectively) vs ϕ graphs in the entire $\cos\theta$ region for ^{12}C-Em interactions 4.5 GeV/c/n
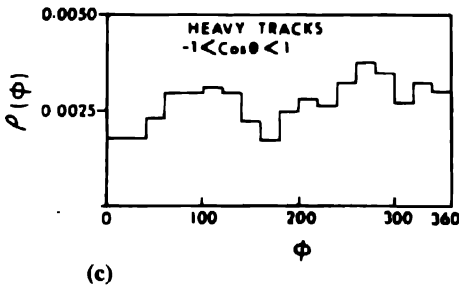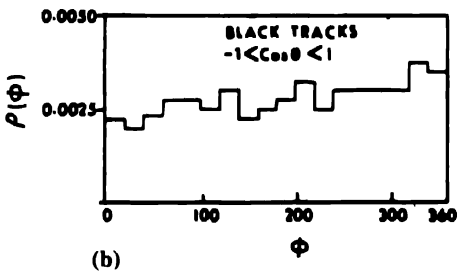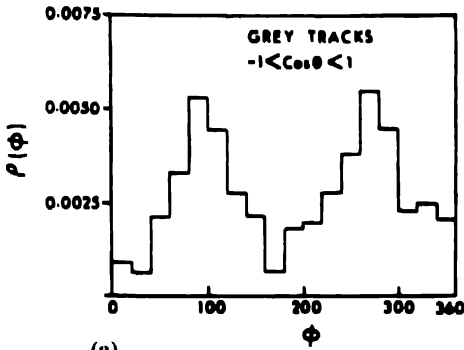
Figure 4. (a) to (c) are plots of normalised $\rho(\phi)$ (for grey, black and heavy tracks respectively) vs ϕ graphs in the entire $\cos\theta$ region for ^{16}O-Em interactions at 60 GeV/c/n.
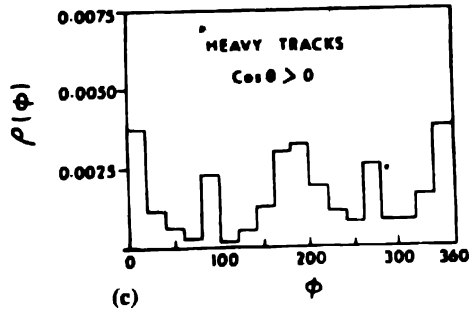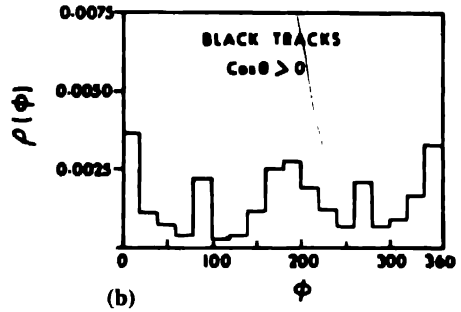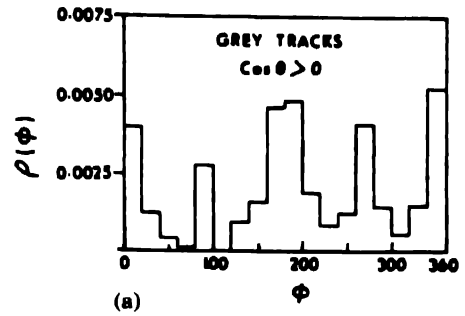
Figure 5. (a) to (c) are plots of normalised $\rho(\phi)$ (for grey, black and heavy tracks respectively) vs ϕ in the forward emission angles ($\theta < 90°$) region for ^{12}C-Em interactions at 4.5 GeV/c/n

the increase of N_h and the observations speak in favour of local heating model of target nucleus. From graphs 2(a) and 2(b), any significant dependence of average azimuthal asymmetry of the black particles on the incident projectile energy is not found. Our data is also consistent with the results of Absemetova *et al* [14] where similar study was made for proton-nucleus interactions at 67–400 GeV.

Here, we added a few more graphs to substantiate our results. We drew normalised azimuthal angle (ϕ) distribution of tracks $\rho(\phi)$ vs ϕ graphs of grey, black and heavy tracks in the entire $\cos\theta$ region for ^{12}C-Em interactions [Figures 3(a) to 3(c)] and ^{16}O-Em interactions [Figures 4(a) to 4(c)] at 4.5 GeV/n/c and 60 GeV/n/c respectively.
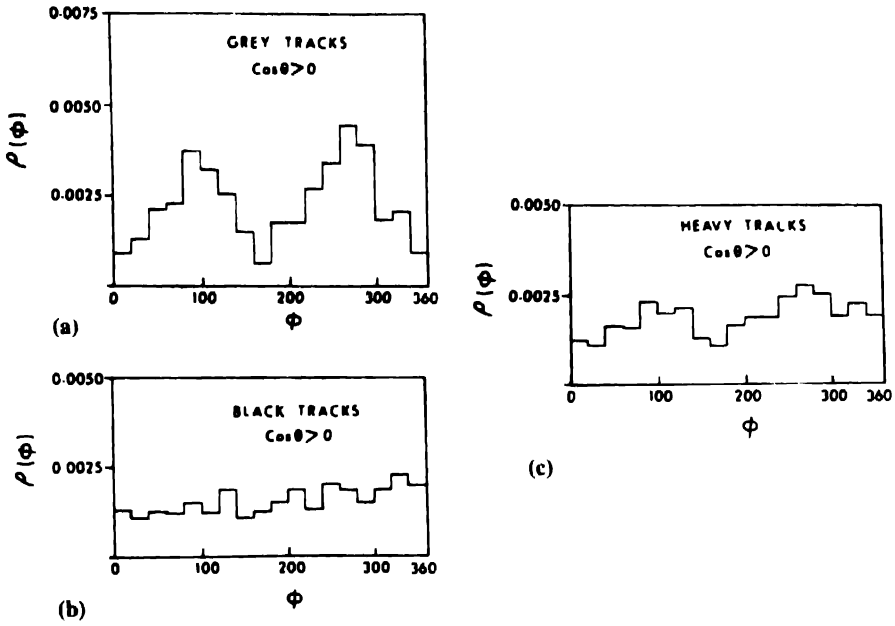
Figure 6. (a) to (c) are plots of normalised $\rho(\phi)$ (for grey, black and heavy tracks respectively) vs ϕ in the forward emission angles ($\theta < 90°$) region for ^{16}O-Em interactions at 60 GeV/c/n.
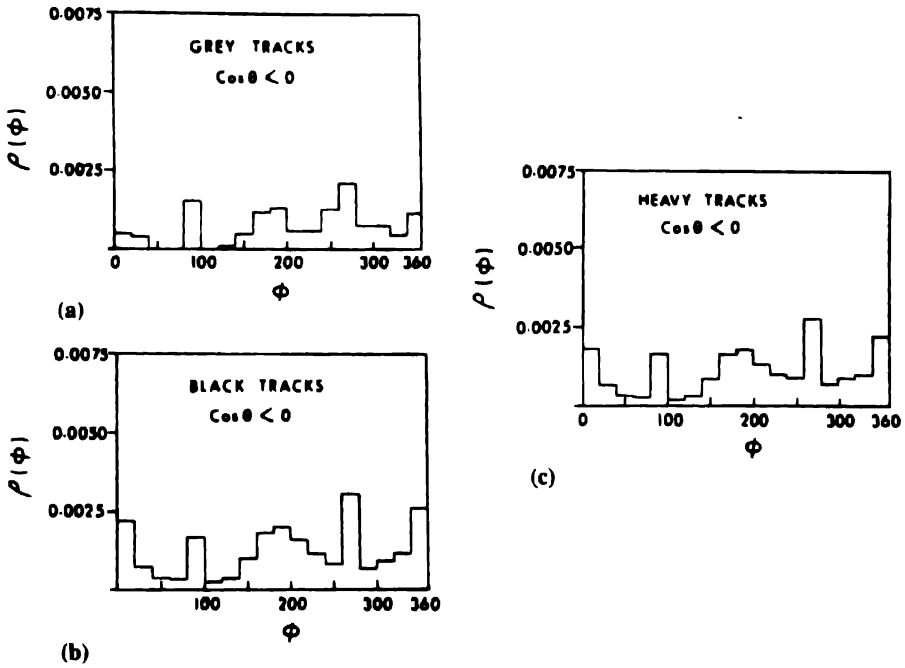

Figure 7. (a) to (c) are plots of normalised $\rho(\phi)$ vs ϕ graphs for grey, black and heavy tracks respectively in the backward emission angles ($\theta > 90°$) region for ^{12}C-Em interactions at 4.5 GeV/c/n.
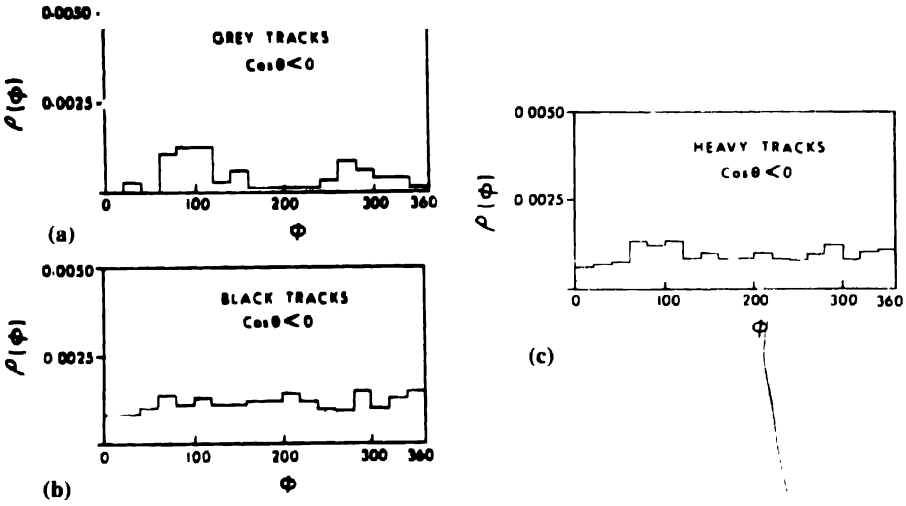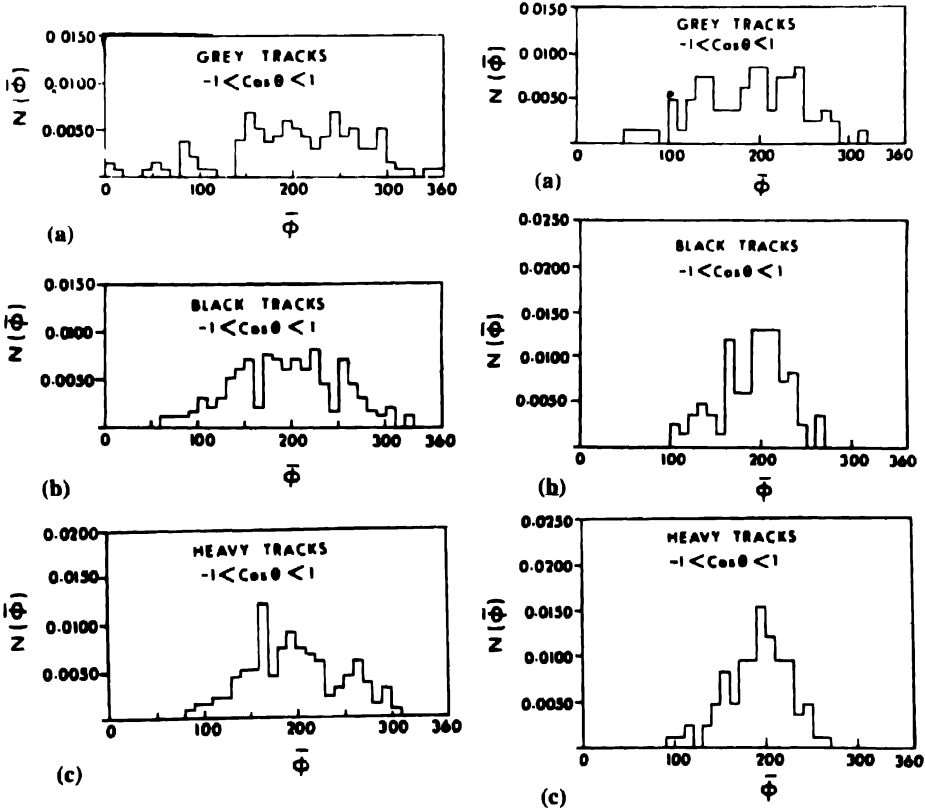
Figure 8. (a) to (c) are plots of normalised $\rho(\phi)$ *vs* ϕ graphs for grey, black and heavy tracks respectively in the backward emission angles ($\theta > 90°$) region for ^{16}O-Em interactions at 60 GeV/c/n

Figure 9. (a) to (c) are plots of normalised $N(\bar{\phi})$ *vs* $\bar{\phi}$ (of grey, black and heavy tracks respectively of an event) in the entire $\cos\theta$ range for ^{12}C-Em interactions at 4.5 GeV/c/n.
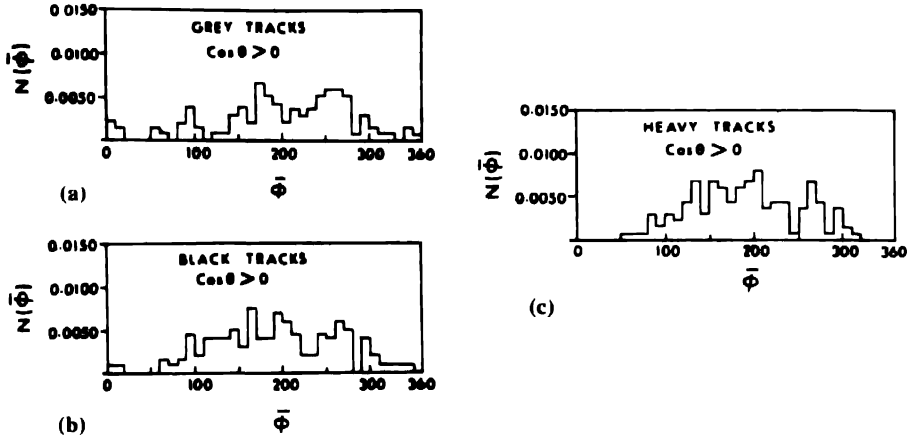
Figure 10. (a) to (c) are plots of normalised $N(\bar{\phi})$ *vs* $\bar{\phi}$ (of grey, black and heavy tracks respectively of an event) in the entire $\cos\theta$ range for ^{16}O-Em interactions at 60 GeV/c/n.
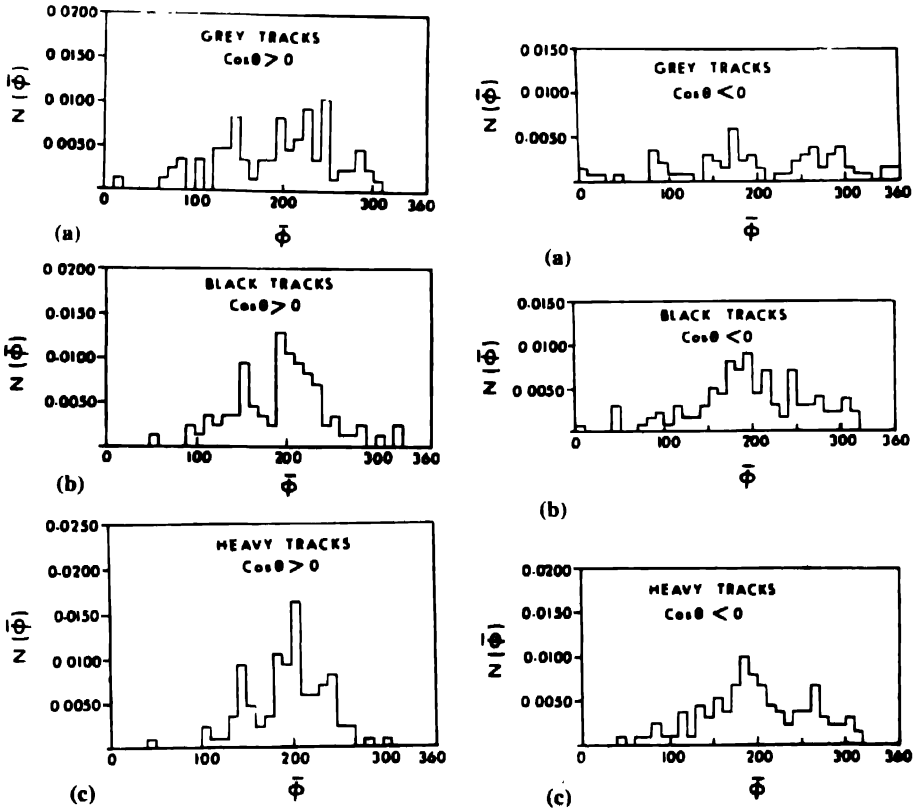
Figure 11. (a) to (c) are plots of normalised $N(\bar{\phi})$ *vs* $\bar{\phi}$ (of grey, black and heavy tracks respectively of an event) in the forward emission angles ($\theta < 90°$) region for ^{12}C-Em interactions at 4.5 GeV/c/n

Figure 12. (a) to (c) are plots of normalised $N(\bar{\phi})$ *vs* $\bar{\phi}$ (of grey, black and heavy tracks respectively of an event) in the forward emission angles ($\theta < 90°$) region for ^{16}O-Em interactions at 60 GeV/n/c.

Figure 13. (a) to (c) are plots of normalised $N(\bar{\phi})$ *vs* $\bar{\phi}$ (of grey, black and heavy tracks respectively of an event) in the backward emission angles ($\theta > 90°$) region for ^{12}C-Em interactions at 4.5 GeV/c/n.

We drew similar plot of $\rho(\phi)$ *vs* ϕ graphs of grey, black and heavy tracks for $\theta < 90°$ (forward emission angles) region [Figures 5(a) to 5(c) for ^{12}C-Em interactions at 4.5 GeV/n/c; Figures 6(a) to 6(c) for ^{16}O-Em interactions at 60 GeV/n/c] and for $\theta > 90°$ (backward emission angles) region [Figures 7(a) to 7(c) for ^{12}C-Em interactions at 4.5 GeV/n/c; Figures 8(a) to 8(c) for ^{16}O-Em interactions at 60 GeV/n/c].

Then we drew normalised $\bar{\phi}$ (averaged over all tracks of the event) distribution $N(\bar{\phi})$ of event for grey, black and heavy tracks of the event *vs* $\bar{\phi}$ [Figures 9(a) to 9(c) for ^{12}C-Em interactions at 4.5 GeV/n/c; Figures 10(a) to 10(c) for ^{16}O-Em interactions at 60 GeV/n/c] in the entire $\cos\theta$ region.
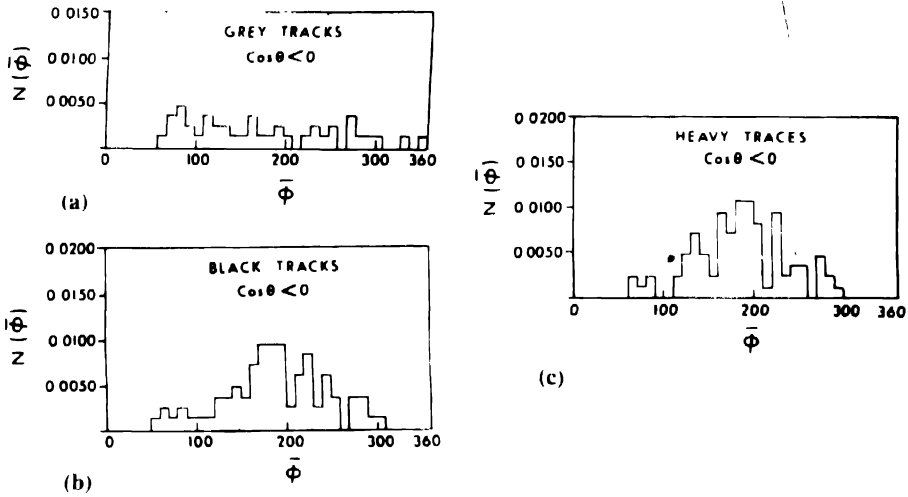

Figure 14. (a) to (c) are plots of normalised $N(\bar{\phi})$ *vs* $\bar{\phi}$ (of grey, black and heavy tracks respectively of an event) in the backward emission angles ($\theta > 90°$) region for ^{16}O-Em interactions at 60 GeV/n/c.

Then we plotted $N(\bar{\phi})$ *vs* $\bar{\phi}$ graphs for grey, black and heavy tracks of event for forward emission angles ($\theta < 90°$) [Figures 11(a) to 11(c) for ^{12}C-Em interactions at 4.5 GeV/n/c; Figures 12(a) to 12(c) for ^{16}O-Em interactions at 60 GeV/n/c] and for backward emission angles $\theta > 90°$ [Figures 13(a) to 13(c) for ^{12}C-Em interactions at 4.5 GeV/n/c; Figures 14(a) to 14(c) for ^{16}O-Em interactions at 60 GeV/n/c] regions.

Acknowledgments

References

[1]   E S Basova *et al Sov. J Nucl Phys* **30** 829 (1979)

[2]   V A Antonchik *et al Sov J Nucl Phys* **46** 790 (1987)

[3]   G D Westfall *et al Phys Rev Lett* **37** 1202 (1976)

[4]   William D Myres *Nucl Phys* **A296** 177 (1978)

[5]   A Bialas *Quark Matter Formation and Heavy Ion Collisions (Proceedings of Bielfeld Workshop, May 1982)* eds M Jacob and H Satz (Singapore · World Scientific) p 139 (1982)

[6]   D Ghosh *et al J Phys* **G20** 1077 (1974)

[7]   James D Sullivan *et al Phys Rev Lett* **30** 136 (1973)

[8]   R Kullberg and I Otterlund Z *Phys* **259** 245 (1973)

[9]   A I Warwick *et al Phys Rev* **C27** 1083 (1983)

[10]   J Gosset *et al Phys Rev* **C16** 629 (1977)

[11]   T Ericson *Adv Phys* **9** 425 (1960), N Dalkhazhaev *et al Sov J Nucl Phys* **23** 643 (1976)

[12]   C F Powell, F Fowler and D H Perkins *Study of Elementary Particles by Photographic Method* (New York Pergamon) (1960)

[13]   D Ghosh *et al Hadron J* **18** 599 (1995)

[14]   Zh A Absemetova *et al Sov J Nucl. Phys.* **42** 909 (1985)